Toxicon 110 (2016) 27–34

Contents lists available at ScienceDirect

Toxicon

journal homepage: www.elsevier.com/locate/toxicon

Bufadienolides from parotoid gland secretions of Cuban toad *Peltophryne fustiger* (Bufonidae): Inhibition of human kidney Na^+/K^+-ATPase activity

Wilmer H. Perera Córdova [a, *], Suzana Guimarães Leitão [a], Geraldino Cunha-Filho [b, 1], Roberto Alonso Bosch [c], Isel Pascual Alonso [c], Rogelio Pereda-Miranda [d], Rodrigo Gervou [b], Natália Araújo Touza [b], Luis Eduardo M. Quintas [b], François Noël [b]

[a] Faculdade de Farmácia, Universidade Federal do Rio de Janeiro, CCS, Bloco A,Ilha do Fundão, 21.941-590 Rio de Janeiro, Brazil
[b] Laboratório de Farmacologia Bioquímica e Molecular, Instituto de Ciências Biomédicas, CCS Bloco J, Ilha do Fundão, 21941-902, Universidade Federal do Rio de Janeiro, Rio de Janeiro, Brazil
[c] Facultad de Biología, Universidad de La Habana, Calle 25 No. 455, Vedado, Havana City, Cuba
[d] Departamento de Farmacia, Facultad de Química, Universidad Nacional Autónoma de México, Ciudad Universitaria, Mexico City, 04510 DF, Mexico

ARTICLE INFO

Article history:
Received 14 July 2015
Received in revised form
24 October 2015
Accepted 18 November 2015
Available online 23 November 2015

Keywords:
Peltophryne fustiger
Western Giant toad
Bufadienolides
1D and 2D NMR spectroscopy
UPLC-MS/MS
HRESIMS
Na^+/K^+ ATPase

ABSTRACT

Parotoid gland secretions of toad species are a vast reservoir of bioactive molecules with a wide range of biological properties. Herein, for the first time, it is described the isolation by preparative reversed-phase HPLC and the structure elucidation by NMR spectroscopy and/or mass spectrometry of nine major bufadienolides from parotoid gland secretions of the Cuban endemic toad *Peltophryne fustiger*: ψ-bufarenogin, gamabufotalin, bufarenogin, arenobufagin, 3-(*N*-suberoylargininyl) marinobufagin, bufotalinin, telocinobufagin, marinobufagin and bufalin. In addition, the secretion was analyzed by UPLC-MS/MS which also allowed the identification of azelayl arginine. The effect of arenobufagin, bufalin and ψ-bufarenogin on Na^+/K^+-ATPase activity in a human kidney preparation was evaluated. These bufadienolides fully inhibited the Na^+/K^+-ATPase in a concentration-dependent manner, although arenobufagin (IC_{50} = 28.3 nM) and bufalin (IC_{50} = 28.7 nM) were 100 times more potent than ψ-bufarenogin (IC_{50} = 3020 nM). These results provided evidence about the importance of the hydroxylation at position C-14 in the bufadienolide skeleton for the inhibitory activity on the Na^+/K^+-ATPase.

Published by Elsevier Ltd.

1. Introduction

Isolation of bioactive compounds from venoms represents an extremely valuable pharmacological approach for the development of animal toxin-based drugs with high specificity and potency towards their molecular targets mainly located in the cardiovascular and nervous systems. As an example, the analgesic properties of the alkaloid epibatidine, isolated from *Epipedobates anthonyi* (Daly, 1998; Fitch et al., 2010), is the result of its binding to nicotinic and muscarinic acetylcholine receptors, while "Chan Su", a mixture of bufadienolides from *Bufo gargarizans* and *Duttaphrynus melanostictus* (also found in literature as *Rhinella gargarizans* and *Rhinella melanostictus*) (Steyn and Heerden, 1998; Chen et al., 2015) has been widely used as a therapeutic agent in China for stimulation of myocardial contraction or the treatment of tonsillitis, sore throat, and palpitations. This traditional crude mixture has also been tested against tumor cell lines and in cancer models (Chan et al., 1995; Steyn and Heerden, 1998; Takai et al., 2012; Lee et al., 2014).

Toad venoms are found in skin secretions (Li et al., 2015) and have been isolated mainly from parotoid glands (Ferreira et al., 2013; Jing et al., 2013; Sciani et al., 2013) of species from the Bufonidae family (Daly et al., 2004), although they have not been detected in the *Melanophryniscus* genus (Mebs et al., 2007). Usually, these secretions contain a wide range of molecules, like biogenic amines, alkaloids, steroids, peptides and high molecular weight proteins (Rash et al., 2011; Tian et al., 2013; Schmeda-Hirschmann

* Corresponding author.
E-mail address: Wilmer.Perera@gmail.com (W.H. Perera Córdova).
[1] We wish to dedicate this work to Geraldino Cunha-Filho who was responsible for most of the Na^+/K^+-ATPase experiments and deceased precociously and abruptly during the writing of this manuscript.

http://dx.doi.org/10.1016/j.toxicon.2015.11.015
0041-0101/Published by Elsevier Ltd.

et al., 2014). These molecules play an important physiological role for anti-microbial defense and against predator attacks (Toledo and Jared, 1995; Jared et al., 2009; Mailho-Fontana et al., 2014). Therefore, parotoid gland venoms are considered a promising reservoir for unexplored active molecules. Among them, cardiac bufadienolides comprise one of the most interesting groups of bioactive substances from secretions of amphibians (Kamboj et al., 2013). They have also been found in reptiles such as the Asian snake *Rhabdophis tigrinus* (Hutchinson et al., 2013) as well as in several plant families (Steyn and Heerden, 1998; Evans, 2002; Mulholland et al., 2009; Kamboj et al., 2013; Zhang et al., 2014). Bufadienolides are C-24 steroids having a 2-pyrone ring linked at C-17 (β-oriented) and a *cis* fusion for both the A/B and C/D ring junctions, and a *trans* fusion for the A/B junction. They are usually characterized by the presence of a 14-β hydroxyl group. Some bufadienolides have been pharmacologically assayed in different *in vitro* and *in vivo* models (Slingerland et al., 2013; Schmeda-Hirschmann et al., 2014). They have shown antitumoral and antiproliferative activity (Tian et al., 2013; Moreno et al., 2013; Ferreira et al., 2013; Schmeda-Hirschmann et al., 2014; Wang and Bi, 2014). Some studies have demonstrated antimicrobial (Cunha-Filho et al., 2010), anti-leishmanial and antitrypanosomal activity (Tempone et al., 2008). The pharmacological effects of bufadienolides were reviewed by Cunha-Filho et al. (2010) and included antiangiogenic, hypertensive or anti-hypertensive, immunosupression, anti-endometriosis and positive ionotropic actions. However, the most relevant pharmacological effect for these steroids is their specific inhibition of Na^+/K^+-ATPase activity (Bagrov et al., 1998; Touza et al., 2011). Some studies have been conducted to establish the structure-activity relationship of bufadienolides as Na^+/K^+-ATPase inhibitors with recent advances comprising the description of the bufalin-Na^+/K^+-ATPase complex using purified porcine kidney enzyme (Tian et al., 2013; Laursen et al., 2015).

Peltophryne fustiger Schwartz, is one of the eight endemic toads from the Cuban archipelago and it is the biggest species among Antillean toads of the family Bufonidae (Alonso et al., 2014). It has a broad distribution in the lowlands and mountains of Western Cuba (Fig. 1A) from the Guanahacabibes Peninsula to the borders of the "Llanura de Zapata", below 390 m elevation (Estrada and Ruibal, 1999). It is a common species that normally inhabits undisturbed areas such as moist broadleaf forests along stream banks in mesic situations and coastal tickets, but it is also found in degraded forest and rural gardens (Díaz and Cádiz, 2008; Henderson and Powell, 2009). Females reach 198.0 mm of snout-vent length, whereas males are smaller with average of 129.5 mm (Schwartz, 1960). Both sexes have large and conspicuous parotoid glands located transversally in a postorbital position on the head (Fig. 1B).

The chemistry of the paratoid gland secretions from Cuban toads has remained unstudied until now. In this study, we focused on the isolation and structural elucidation of the major bufadienolides from the parotoid gland secretions of the *P. fustiger* and the evaluation of the inhibitory effect of three of them on human kidney Na^+/K^+-ATPase activity.

2. Materials and methods

2.1. Secretion collection and extraction

Parotoid gland secretions were collected from seven adult male specimens of *P. fustiger* in Santo Tomás stream, El Moncada, Viñales, Pinar del Río, Cuba (22°33′00.8″N 83°50′14.6″W) on March, 29, 2014. The secretions were obtained by mechanical compression of both glands from living individuals. These yellowish and doughy secretions were collected on a surface of a watch glass. After this procedure, the individuals were released; only one specimen was preserved as a voucher and deposited in the Herpetological Collection of the Museum of Natural History "Felipe Poey", Faculty of Biology, University of Havana, Cuba (MFP 11.599).

Fresh secretions (1.45 g) were extracted three times with 80 mL MeOH by shaking at room temperature. Extract solutions were pooled, filtered and evaporated under reduced pressure to afford 266 mg of a pale yellowish crude extract.

2.2. HPLC analyses

2.2.1. Analytical conditions

20 μL (2 mg/mL) of crude extract were injected in a RP C-18 Purospher, Merck Millipore (250 × 4 mm, 5 μm) column at 30 °C. The elution was performed using gradient of 0.1% trifluoroacetic acid (A) and acetonitrile (B) as follows: 0–10 min, 5% B; 10–20 min, 5–40% B; 20–25 min, 40% B; 25–60 min, 40–70% B. The flow rate was set at 1 mL/min and the chromatogram was analyzed mainly at 300 nm.

2.2.2. Preparative conditions

250 mg of crude extracts were dissolved in 8 mL of MeOH and filtered through 0.45 μm Minisart RC 4 filters. 300 μL of the sample were successively subjected to preparative HPLC Dionex Ultimate 3000 on a Phenomenex Luna RP-C18 (250 mm × 21.2 mm, 10 μm) by using gradient of elution as follows: 0–10 min, 5% B; 10–20 min,

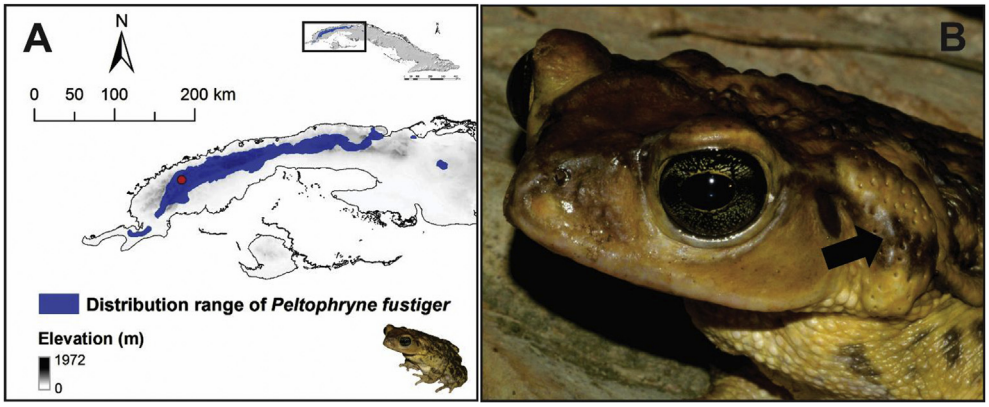

Fig. 1. (A) Shaded area represents the approximate distribution range of *Peltophryne fustiger* in Western Cuba. Red dot indicates the collection locality (B) Details of the head of an adult male of this species, with the arrow indicating the large parotoid gland. Photograph courtesy of J. Bosch. (For interpretation of the references to color in this figure legend, the reader is referred to the web version of this article.)

5–30% B; 20–25 min, 30% B; 25–50 min, 30–50% B and 50–55 min, 50–100% B. The flow rate was 15 mL/min, and the detection wavelength was fixed at 300 nm. HPLC analyses led the isolation of ten compounds: **7** (23.52 min, < 1 mg); **10** (27.02 min, 6.7 mg); **11** (28.82 min, < 1 mg); **12** (29.21 min, 1.8 mg); **14** (34.02 min, 22.2 mg); **15** (39.18 min, < 1 mg); **16** (42.03 min, < 1 mg); **17** (46.0 min, 10.3 mg); **18** (50.02 min, 12.8 mg), **19** (53.3 min, 2 mg). Compounds **10** and **14** were further purified by using the same column and chromatographic conditions to afford both chemicals with relative purities higher than 97%.

2.3. Spectroscopic and spectrometric analyses

Spectra were recorded on a Bruker Avance 500 NMR spectrometer at 298 K, operating at 500.13 MHz for ^{1}H and 125.75 MHz for ^{13}C using MeOH-d_4 and $CHCl_3$-*d*. Chemical shifts were reported in δ (ppm) relative to tetramethylsilane, used as an internal standard. Coupling constants were reported as *J* (Hz) and multiplicities with abbreviations *d*, doublet; *dd*, doublet of doublets and *br*, broad signal. HRESIMS and ESI-MS/MS spectra were recorded on an ESI-Qq-TOF mass spectrometer (micrOTOF-Q III, Bruker) and in a Bruker Ion Trap Mass Spectrometer respectively, both in the positive ion mode by direct infusion.

2.4. UPLC-MS/MS analysis

Analyses were performed in an Acquity UPLC system (Waters). 10 μL (1 mg/mL MeOH:H_2O (1: 1; v:v) were injected in a RP-C18 (2.1 × 50 mm, 1.7 μm) Waters Acquity UPLC BEH using a gradient elution of 0.1% formic acid (A) and acetonitrile (B) 0–8 min 15–100% (B). The flow rate was set at 0.3 mL/min and the chromatogram recorded in the range of 190–400 nm. MS data were measured using an electrospray ionization source coupled to a SQD system (Waters) in both positive and negative ionization modes: ESI conditions. Positive mode: capillary (3.5 kV); cone (30 V); desolvation temp (350 °C); desolvation gas (300 L/Hr); sweep gas, 5. Negative mode: capillary (4.0 kV); cone (40 V); desolvation temp (350 °C); desolvation gas (300 L/Hr); sweep gas, 5. Mass range was set to optimally pass ions from *m*/*z* 100–2000.

2.5. Preparation of Na^+/K^+-ATPase from human kidney

Normal human renal tissues (from the unaffected pole) were obtained from patients who underwent unilateral nephrectomy due to well-encapsulated hypernephroma in one kidney pole. All procedures for the use of discarded organ portions were performed in accordance with the Institutional Ethical Committee from Hospital Universitário Clementino Fraga Filho, Universidade Federal do Rio de Janeiro, Brazil.

Crude homogenate preparations were obtained according to previously described procedures (Quintas et al., 1997; Lopez et al., 2002). Briefly, the tissue was homogenized in a Potter homogenizer with a motor driven Teflon pestle at 4 °C in 2–3 volumes of ice cold 0.25 M buffered sucrose pH 7.4, containing 0.1 mM phenylmethylsulfonyl fluoride (PMSF) per gram organ. After centrifugation at 100,000g for 1 h, pellets were re-suspended with the same buffer without PMSF and were stored in N_2 until use. The protein concentration was measured according to the method of Lowry et al. (1951) using bovine serum albumin as the standard.

2.6. Inhibition of Na^+/K^+-ATPase activity

The Na^+/K^+-ATPase activity was determined by the Fiske and Subbarow method (1925) with slight modifications, as previously described (Pôças et al., 2007). The specific activity of the enzyme corresponds to the difference between the total ATPase activity and the activity measured in the presence of 1 mM ouabain. The preparation was incubated at 37 °C for 2 h, in 0.5 mL of 84 mM NaCl, 3 mM KCl, 3 mM $MgCl_2$, 1.2 mM $ATPNa_2$, 2.5 mM EGTA, 10 mM sodium azide and 20 mM maleic acid buffered with TRIS to pH 7.4 in the absence or presence of inhibitor(s). Classical concentration–effect (dose–response) curves were performed with each inhibitor. Crude extract and selected compounds were evaluated and results were expressed as half-maximal inhibitory concentration (IC_{50}).

2.7. Statistical analysis

2.7.1. Concentration-effect curves for inhibition of Na^+/K^+-ATPase activity

Inhibition curves were fitted using computerized non-linear regression analysis of the data (Prism®, GraphPad Software Inc., version 5.01), assuming a sigmoidal dose–response curve model, where the parameters bottom and top were fixed at 0 and 100%, respectively, to determine the half maximal inhibitory concentration (IC_{50}), as previously reported for a similar study (Pôças et al., 2007). For illustrative purpose, mean curves form 3–4 independent experiments are shown in the figures but the IC_{50} values in the text are expressed as geometric means of the different experiments with their 95% confidence interval.

3. Results

3.1. Isolation and structure elucidation

The DAD-RP-HPLC chromatographic profile of the crude extract from parotoid gland secretions of *P. fustiger* (Fig. 2) was mainly composed of peaks with UV-spectra, *ca.* 214 and 300 nm (Fig. 2A) characteristics of the 2-pyrone chromophore of the bufadienolides (Liu et al., 2010).

Taking into account that most of the signals showed the characteristic UV spectrum of bufadienolides, and the molar absorptivity of this subfamily of compounds are quite similar, it was recognized that peaks 14, 17 and 18 represented the major compounds in the crude extracts. The scale up to preparative RP-HPLC

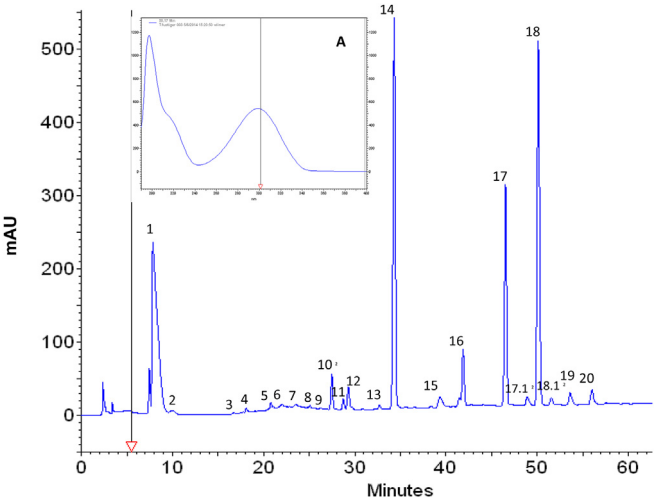

Fig. 2. Analytical RP-C18 HPLC chromatographic profile of crude extract from parotoid gland secretion of *Peltophryne fustiger* recorded at 300 nm. (**7**) Azelayl arginine (**10**) ψ-bufarenogin, (**11**) gamabufotalin, (**12**) bufarenogin, (**14**) arenobufagin, (**15**) 3-(*N*-suberoylargininyl) marinobufagin, (**16**) bufotalinin, (**17**) telocinobufagin, (**18**) marinobufagin, (**19**) bufalin: UV-spectrum of marinobufagin) (**A**).

was successfully achieved despite the fact that analytical and preparative C-18 stationary phases were manufactured by different companies. Similar analytical and preparative chromatograms were registered. Thus, the application of this methodology allowed the isolation of ten compounds.

Compounds **10**, **12**, **14, 17, 18** and **19** were identified as ψ-bufarenogin, bufarenogin, arenobufagin, telocinobufagin, marinobufagin and bufalin, respectively, by comparison of their NMR and MS data with those previously reported in literature (Kamano et al., 1998; Ye and Guo, 2005; Ye et al., 2006; Cunha-Filho et al., 2010). ^{1}H and ^{13}C chemical shifts were unambiguously assigned by $^{1}H–^{1}H$ COSY, HSQC and HMBC, and summarized in Tables 1 and 2. The minor constituents from the analyzed venom were tentatively identified by UPLC-MS/MS, in the positive and negative ion modes (Table 3), as azelayl arginine **(7)**, gamabufotalin **(11)**, 3-(*N*-suberoylargininyl)-marinobufagin **(15)**, and bufotalinin **(16)**, by comparison of retention times, UV spectra and MS data with those reported in literature (Gao et al., 2010; Schmeda-Hirschmann et al., 2014). Chemical structures of the isolated compounds are shown in Fig. 3.

3.2. Inhibition of human kidney Na^{+}/K^{+}-ATPase

The methanolic extract of the *P. fustiger* venom fully inhibits the Na^{+}/K^{+}-ATPase activity present in a human kidney membrane preparation, in a concentration-dependent manner (Fig. 4A), with a IC_{50} value of 0.468 μg/ml (95% CI: 0.207–1.060). Particularly, pure arenobufagin, bufalin and ψ-bufarenogin isomers also fully inhibit Na^{+}/K^{+}-ATPase activity (Fig. 4B). However, arenobufagin [IC_{50} value: 28.3 nM (95% CI: 7.93–101)] and bufalin [IC_{50} value: 28.7 nM (95% CI: 13.6–60.5)] were 100 times more potent than ψ-bufarenogin [IC_{50} value: 3020 nM (95% CI: 2189–4167)].

4. Discussion

The composition and pharmacological properties of the secretions from parotoid glands and skin of members of the Bufonidae family have been studied for a long time (Chen and Chen, 1933). One of the earlier contributions summarized 50 compounds from 39 species collected from several localities worldwide (Low, 1972). More than forty years later, herein we present the isolation of the first bufadienolides from Antillean endemic bufonids, specifically from the Cuban Giant toad *P. fustiger*. The compounds (Fig. 3) are among the most commonly isolated bufadienolides from species of this family (Cunha-Flho et al., 2005, 2010; Sciani et al., 2013; Qi et al., 2014). However, only one of them (marinobufagin) has been identified in species of the genus *Rhaebo* (Ferreira et al., 2013), one of the closest relative lineages of *Peltophryne* (Van Bocxlaer

Table 1
^{1}H NMR chemical shifts of bufadienolides isolated from parotoid gland secretions of *Peltophryne fustiger*.

^{1}H	ψ-bufarenogin (10) δ ppm	Bufarenogin (12) δ ppm	Arenobufagin (14) δ ppm	Telocinobufagin (17) δ ppm	Marinobufagin (18) δ ppm	Bufalin (19) δ ppm
1	1.76 (m, 1H) 1.58 (m, 1H)		2.39 (m, 1H) 1.48 (m, 1H)	1.81 (m, 1H) 1.38 (m, 1H)	1.83 (m, 1H) 1.40 (m, 1H)	1.49 (m, 1H) 1.42 (m, 1H)
2	1.87 (m, 1H) 1.68 (m, 1H)		1.72 (m, 1H) 1.51 (m, 1H)	1.70 (m, 1H) 1.59 (m, 1H)	1.65 (m, 1H) 1.61 (m, 1H)	1.58 (m, 1H) 1.52 (m, 1H)
3	4.20 (br, s, 1H)	4.03 (br, s, 1H)	4.13 (br, s, 1H)	4.14 (br, s, 1H)	4.12 (br, s, 1H)	4.14 (br, s, 1H
4	1.80 (m, 1H) 1.48 (m, 1H)		1.79 (m, 1H) 1.37 (m, 1H)	2.24 (m, 1H) 1.48 (m, 1H)	2.25 (m, 1H) 1.46 (m, 1H)	1.88 (m, 1H) 1.35 (m, 1H)
5	1.88 (m, 1H)		1.86 (m, 1H)	–	–	1.75 (m, 1H)
6	1.96 (m, 1H) 1.40 (m, 1H)		1.95 (m, 1H) 1.33 (m, 1H)	1.73 (m, 1H) 1.39 (m, 1H)	1.69 (m, 1H) 1.30 (m, 1H)	1.88 (m, 1H) 1.27 (m, 1H)
7	1.87 (m, 1H) 1.30 (m, 1H)		1.81 (m, 1H) 1.37 (m, 1H)	1.95 (m, 1H) 1.27 (m, 1H)	1.62–1.60 (m, 2H)	1.72–1.18 (m, 2H)
8	2.37 (m, 1H)		2.02 (m, 1H)	1.67 (m, 1H)	2.42 (m, 1H) 1.96 (m, 1H)	1.51 (m, 1H)
9	2.46 (d, 1H) J = 12.2 Hz	2.79 (d, 1H)	1.75 (m, 1H)	1.62 (m, 1H)	1.65 (m, 1H)	1.61 (m, 1H)
10	–	–	–	–	–	–
11	–		4.33 (d, 1H) J = 11.2 Hz	1.48 (m, 1H) 1.30 (m, 1H)	1.63 (m, 1H) 1.43 (m, 1H)	1.72–1.18 (m, 2H)
12	4.11 (s, 1H)	4.06 (s, 1H)	–	1.52 (m, 1H) 1.46 (m, 1H)	1.72 (m, 1H) 1.51 (m, 1H)	1.49 (m, 1H) 1.39 (m, 1H)
13	–	–	–	–	–	–
14	–	–	–	–	–	–
15	1.68 (m, 1H) 1.55 (m, 1H)		1.75 (m, 1H) 1.35 (m, 1H)	2.09 (m, 1H) 1.72 (m, 1H)	3.60 (s. 1H)	2.06 (m, 1H) 1.69 (m, 1H)
16	1.88 (m, 1H) 1.69 (m, 1H)		2.05 (m, 1H) 1.73 (m, 1H)	2.21 (m, 1H) 1.73 (m, 1H)	1.66 (m, 1H) 1.31 (m, 1H)	2.18 (m, 1H) 1.72 (m, 1H)
17	2.36 (m, 1H)		4.10 (m, 1H)	2.58 (dd, 1H) J = 9.4, 6.1 Hz	2.59 (br, d, 1H)	2.46 (m, 1H)
18	1.05 (s, 3H)	1.24 (s, 3H)	0.93 (s, 3H)	0.73 (s, 3H)	0.74 (s, 3H)	0.70 (s, 3H)
19	1.0 (s, 3H)	0.50 (s, 3H)	1.19 (s, 3H)	0.95 (s, 3H)	1.0 (s, 3H)	0.95 (s, 3H)
20	–	–	–	–	–	–
21	7.33 (d, 1H) J = 2.6 Hz	7.46 (d, 1H) J = 2.6 Hz	7.39 (d, 1H) J = 2.4 Hz	7.45 (d, 1H) J = 2.4 Hz	7.48 (d, 1H) J = 2.4 Hz	7.24 (d, 1H) J = 2.6 Hz
22	7.49 (dd, 1H) J = 9.7; 2.6 Hz	7.93 (dd, 1H) J = 9.8, 2.5 Hz	7.71 (dd, 1H) J = 9.7; 2.4 Hz	8.01 (dd, 1H) J = 9.7, 2.3 Hz	7.90 (dd, 1H) J = 9.7, 2.4 Hz	7.85 (dd, 1H) J = 9.7, 2.6 Hz
23	6.26 (d, 1H) J = 9.7 Hz	6.28 (d, 1H) J = 9.6 Hz	6.29 (d, 1H) J = 9.7 Hz	6.30 (d, 1H) J = 9.7 Hz	6.26 (d, 1H) J = 9.7 Hz	6.26 (d, 1H) J = 9.7 Hz
24	–	–	–	–	–	–

Assignments were made by analysis of COSY, HSQC, HMBC and/or NOESY spectra. Overlapping signals are reported without designating multiplicity.
Chemical shifts of ψ-bufarenogin, arenobufagin and bufalin are presented in $CHCl_3$-*d* whereas for bufarenogin, telocinobufagin, marinobufagenin are shown in MeOH-d_4.

Table 2
^{13}C NMR chemical shifts in $CHCl_3$-d and MeOH-d_4 of five bufadienolides isolated from parotoid gland secretions of *P. fustiger*.

^{13}C	ψ-bufarenogin (10) δ ppm			Arenobufagin (14) δ ppm			Telocinobufagin (17) δ ppm			Marinobufagin (18) δ ppm			Bufalin (19) δ ppm		
	$CHCl_3$-d	MeOH-d_4	Δ	$CHCl_3$-d	MeOH-d_4	Δ	$CHCl_3$-d	MeOH-d_4	Δ	$CHCl_3$-d	MeOH-d_4	Δ	$CHCl_3$-d	MeOH-d_4	Δ
1	29.65	29.51	+0.14	31.72	31.59	+0.13	24.82	24.72	+0.10	24.76	24.64	+0.12	29.62	29.40	+0.22
2	28.22	27.55	**−0.67**	28.63	27.74	**+0.89**	27.96	27.07	**+0.89**	27.91	27.06	**+0.85**	27.86	27.13	**+0.73**
3	66.47	65.95	**+0.52**	66.79	66.37	+0.42	68.08	67.66	+0.42	68.0	67.61	+0.39	66.85	66.27	**+0.58**
4	33.98	33.13	**+0.85**	33.49	33.04	+0.45	36.86	36.32	**+0.54**	36.85	36.28	**+0.57**	33.26	32.75	**+0.51**
5	36.17	36.38	−0.21	37.59	37.79	−0.20	74.64	74.78	−0.14	74.62	74.39	+0.23	35.96	36.02	−0.06
6	26.88	26.88	–	26.34	26.28	+0.06	35.31	34.53	**+0.78**	34.65	33.75	**+0.90**	26.51	26.47	+0.04
7	20.74	20.61	+0.13	21.69	21.34	+0.35	23.81	23.38	+0.43	23.25	22.56	**+0.69**	21.40	21.17	+0.23
8	39.29	39.45	−0.16	39.71	39.29	+0.42	41.44	40.60	**+0.84**	32.60	31.73	**+0.87**	42.33	41.60	**+0.73**
9	46.45	46.34	+0.11	40.62	39.90	**+0.72**	39.23	38.74	+0.49	42.73	42.42	+0.31	35.37	35.06	+0.31
10	38.38	37.64	**+0.74**	37.04	36.72	+0.32	40.92	40.50	+0.42	40.87	40.60	+0.27	35.67	35.45	+0.22
11	214.27	214.40	−0.13	73.45	73.78	−0.33	21.77	21.60	+0.17	21.42	21.24	+0.18	21.40	21.17	+0.23
12	82.57	82.56	−0.01	213.74	213.76	−0.02	40.92	40.50	+0.42	39.38	38.67	**+0.71**	40.91	40.54	+0.37
13	54.29	54.30	−0.01	61.75	62.47	**−0.72**	49.09	47.58	**+1.51**	45.04	44.73	+0.31	48.36	48.37	−0.01
14	83.18	82.92	+0.26	85.71	85.05	**+0.66**	84.47	84.65	−0.18	74.76	74.68	+0.08	85.39	84.76	**+0.63**
15	33.79	33.32	+0.47	32.92	31.74	+1.18	32.66	31.73	**+0.93**	59.77	59.77	–	32.71	31.79	**+0.92**
16	27.33	27.21	+0.12	27.93	27.64	+0.29	28.58	28.36	+0.22	32.31	32.67	−0.36	28.73	28.46	+0.27
17	45.48	45.54	−0.06	40.83	40.51	+0.32	51.06	50.69	+0.37	47.58	47.24	+0.34	51.21	50.88	+0.33
18	19.39	17.87	**+1.52**	17.45	16.72	**+0.73**	16.44	15.83	**+0.61**	16.76	15.64	**+1.12**	16.53	15.93	**+0.60**
19	24.26	23.39	**+0.87**	23.38	22.58	**+0.80**	16.69	15.83	**+0.86**	16.76	15.85	**+0.91**	23.73	22.91	**+0.82**
20	118.96	120.31	**+1.55**	120.46	121.97	**−1.51**	122.35	123.62	**−1.27**	122.14	123.09	**−0.95**	122.78	123.67	**−0.89**
21	150.66	151.13	+0.47	150.04	150.24	−0.20	148.60	149.09	−0.49	149.58	150.37	**−0.79**	148.52	149.04	**−0.52**
22	146.95	148.41	**+1.46**	146.38	148.09	**−1.71**	146.62	147.96	**−1.34**	146.91	148.16	**−1.25**	146.90	147.99	**−1.09**
23	114.66	113.11	**+1.55**	115.77	114.48	**+1.29**	115.42	114.02	**+1.40**	115.33	113.96	**+1.37**	115.27	114.02	**+1.25**
24	162.03	163.22	**−1.19**	162.06	163.71	**−1.65**	162.78	163.44	**−0.66**	162.04	163.09	**−1.05**	162.49	163.43	**−0.94**

Δ: Difference between chemical shifts in $CHCl_3$-*d* − MeOH-d_4; Assignments were made by analysis of COSY, HSQC, and HMBC spectra.
Bold means difference in chemical shifts higher than 0.5 ppm.

Table 3
Tentative identification of minor constituents from *Peltophryne fustiger* venom by UPLC-MS/MS in the negative and positive ion modes based on Gao et al. (2010) and Schmeda-Hirschmann et al. (2014).

Compound	$[M-H]^-$	$[M+H]^+$	UV trace	Tentative identification	Main fragments[a]
7	343.2	345.3	No bufadienolide	Azelayl arginine	250.2; 175.1 (arginine)
11		403.3	Bufadienolide	Gamabufotalin	425.3 (M + Na); 385.4 (M + H−H_2O); 331.3 (385−2x H_2O)
15	711.5	713.1	Bufadienolide	3-(*N*-suberoylargininyl) Marinobufagin (Marinobufotoxin)	695.7 (M + H−H_2O); 331.3; 287.3; 250.2; 175.2 (arginine)
16	413.2	415.2	Bufadienolide	Bufotalinin	437.3 (M + Na); 397.3 (M + H−H_2O); 385.4 (M + H−H_2CO); 331.3

[a] Positive ion mode: (MS/MS).

et al., 2010; Alonso et al., 2012). To the best of our knowledge, this is the first report about toad venoms showing arenobufagin as the major compound.

The IC_{50} values obtained for arenobufagin and bufalin were similar to those previously reported by us for telocinobufagin (Touza et al., 2011) all tested with human kidney enzyme under the same experimental conditions (Table 4), and also equivalent to the value reported for bufalin using a porcine kidney enzyme preparation (Laursen et al., 2015). These authors also described the structure of the bufalin-porcine kidney Na^+/K^+-ATPase complex in the presence of K^+ (Laursen et al., 2015). This complex is structurally similar to the digoxin-Na^+/K^+-ATPase complex obtained in the same work, and also to the ouabain-Na^+/K^+-ATPase complex described previously (Laursen et al., 2013), indicating a similar mechanism of Na^+/K^+-ATPase inhibition by cardenolides and bufadienolides. Specifically, the hydroxyl substituent at C-14 of bufalin (highly conserved among bufadienolides) is within hydrogen-bond distance to Thr797 (αM6) and further stabilized by Asp121 (αM2) in the porcine enzyme complex. With respect to the lactone group, the six-membered lactone of bufalin reached deeper into the cation-binding site of the porcine enzyme than ouabain and digoxin (Laursen et al., 2013, 2015). This binding mode for bufalin indicated the relevance of the hydroxyl at C-14 and the six-membered lactone moiety, in the inhibition of the porcine Na^+/K^+-ATPase. Since human and porcine Na^+/K^+-ATPase share 98.1% of sequence identity, the inhibition of the human kidney enzyme by bufalin, telocinobufagin and arenobufagin (bufadienolides sharing similar IC_{50} values) probably follow a similar mechanism to that described for the interaction of bufalin with the porcine enzyme.

Moreover, the substitution of the OH at C-14 (well conserved in the bufadienolide family) in marinobufagin by an epoxy group comprising cyclization of hydroxyl group between C-14 and C-15, also has a profound negative effect on the inhibition of the human kidney enzyme with IC_{50} value around 25–40 fold higher in comparison with arenobufagin, bufalin and telocinobufagin (Touza et al., 2011) (Table 4). These results are in good agreement with the binding mode of bufalin:porcine kidney Na^+/K^+-ATPase complex.

Additionally, the results suggest that the presence of a ketone group at C-12 and a hydroxyl at C-11 on arenobufagin had no effect on the inhibitory potency regarding bufalin and telocinobufagin. However, interchanging the position of these two substituents promotes an important decrease in the inhibitory potency, since the IC_{50} of ψ-bufarenogin was 100-fold higher (Table 4). We can

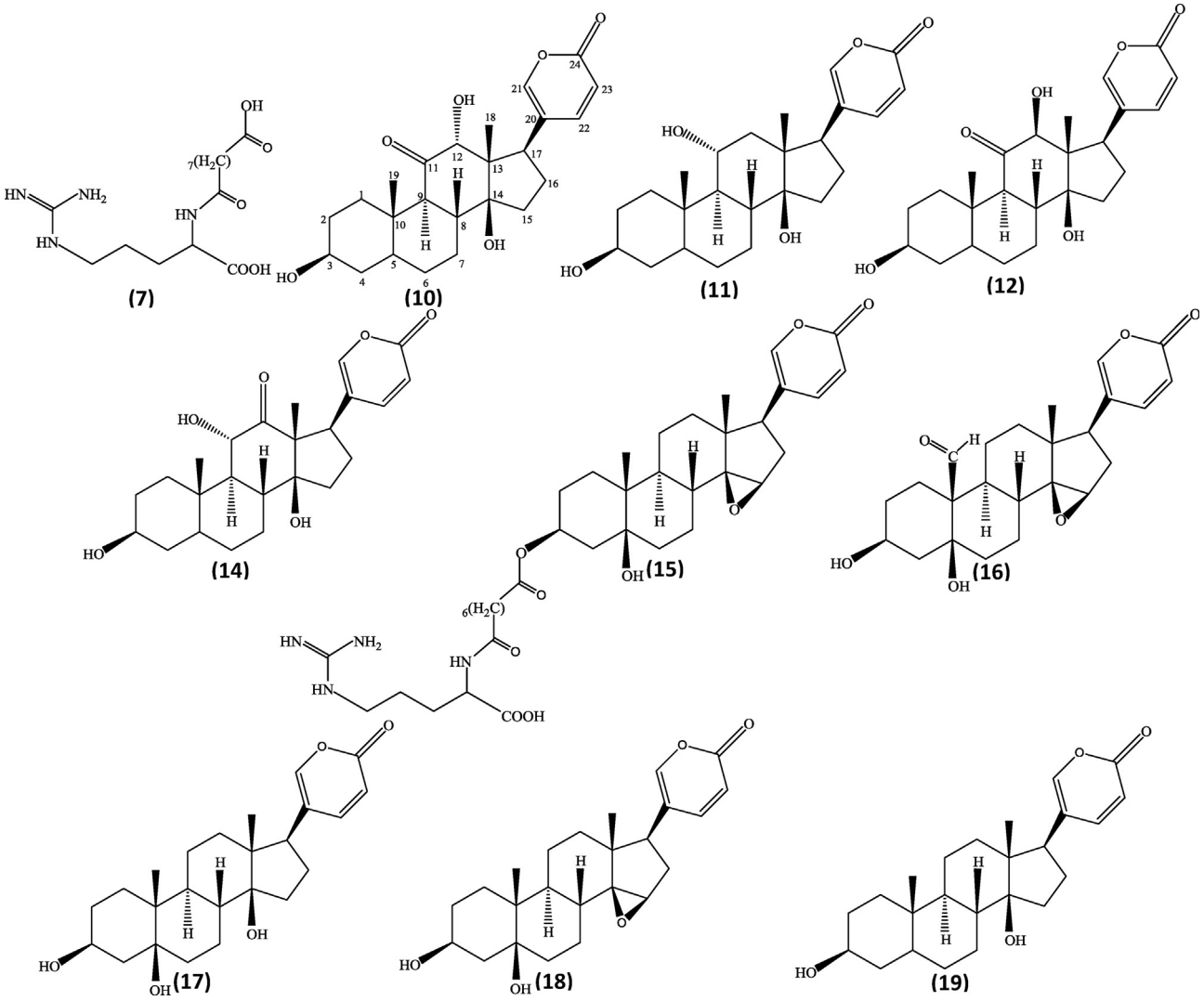

Fig. 3. Chemical structures of the compounds from *P. fustiger*. The numbers correspond with the elution order in the analytical RP-C18 column as in Fig. 2: **(7)** Azelayl arginine **(10)** ψ-bufarenogin, **(11)** gamabufotalin, **(12)** bufarenogin, (**14**) arenobufagin, **(15)** 3-(*N*-suberoylargininyl) marinobufagin, **(16)** bufotalinin, **(17)** telocinobufagin, (**18**) marinobufagin, **(19)** bufalin.

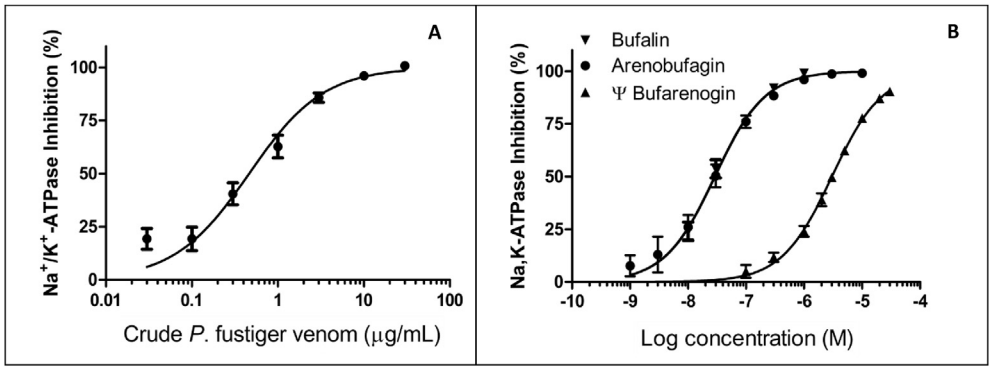

Fig. 4. Inhibition curves of Na^+/K^+-ATPase activity from human kidney preparation: (A) methanolic extract from parotoid gland secretion from *P. fustiger*; (B) bufalin, arenobufagin, and ψ-bufarenogin. Results (mean ± SEM) were expressed as percent of the inhibition measured in the presence of 1 mM ouabain; A (n = 4) and B (n = 3).

hypothesize that the more rigid ketone group at C-11 position in ψ-bufarenogin is less well accommodated in the enzyme in comparison with the same group on C-12 position in arenobufagin.

5. Conclusions

The chemical analyses of parotoid gland secretions of the

Table 4
Summary of the substituents on the steroid core of different bufadienolides, and their corresponding IC_{50} for inhibition of Na^+/K^+-ATPase enzymatic activity from human kidney.

Bufadienolide	Substituents at the steroid core						IC_{50} (nM)	Reference
	3β	5β	11	12	14β	19β		
arenobufagin	OH	H	α-OH	C=O	OH	CH_3	28.3	Present work
bufalin	OH	H	H	H	OH	CH_3	28.7	Present work
Ψ-bufarenogin	OH	H	C=O	β-OH	OH	CH_3	3020	Present work
marinobufagin	OH	OH	H	H	14-O-15 epoxide	CH_3	1144	Touza et al., 2011
telocinobufagin	OH	OH	H	H	OH	CH_3	44.2	Touza et al., 2011

In all cases, the IC_{50} values were determined under the same experimental conditions in presence of 3.0 mM KCl.

Western Giant toad *P. fustiger* from Cuba led the isolation and structure elucidation of the metabolites azelayl arginine, ψ-bufarenogin, gamabufotalin, bufarenogin, arenobufagin, 3-(*N*-suberoylargininyl) marinobufagin, bufotalinin, telocinobufagin, marinobufagin and bufalin. This is the first report of the occurrence of bufadienolide steroids and azelayl arginine not only in the *P. fustiger*, but also among the Antillean toads of this genus. It is also noteworthy that arginine bufadienolide esters are present only in very small amounts. Arenobufagin, the main component of the secretion, showed a potent inhibition of human kidney Na^+/K^+-ATPase (IC_{50} in the nM range). The integration of the present data with recent findings on the structure of the bufalin-porcine enzyme complex confirms that the presence of a hydroxyl group at position C-14 in bufadienolides (also conserved in cardenolides), is highly important for a tight binding of these compounds to the Na^+/K^+-ATPase.

Ethical statement

On behalf of, and having obtained permission from all the authors, Wilmer H. Perera Córdova declares that the manuscript has not been published elsewhere or under editorial review for publication elsewhere; and all the co-authors of the research are fully aware of this submission.

Conflict of interest

The authors declare that there are no conflicts of interest and certify that this paper consists of original, unpublished work, which is not under consideration for publication elsewhere.

Acknowledgments

The authors are grateful to CAPES and FAPERJ for the post-doctoral support to WHPC and GCF. We also thank CNRMN-National Center of Nuclear Magnetic Resonance Jiri Jonas from Federal University of Rio de Janeiro for kindly allowing us to record the NMR spectra as well as Dr. Ari Miranda da Silva and Marina Amaral for HRESI and ESI mass spectrometric measurements. FN and LEMQ are research fellows from CNPq and RG is a student fellow from PIBIC-EM/CNPq. R.P.-M. was a visiting research scientist at Faculdade de Farmácia, Universidade Federal do Rio de Janeiro with partial financial support from Dirección General de Asuntos del Personal Académico, UNAM. We also thanks Ms. Vanessa Dias for helping us with some experiments. We wish to thank L.Y. Garcia for his assistance in the fieldwork and Dr. James D. McChesney for checking the English grammar.

Appendix A. Supplementary data

Supplementary data related to this article can be found at http://dx.doi.org/10.1016/j.toxicon.2015.11.015.

Transparency document

Transparency document related to this article can be found online at http://dx.doi.org/10.1016/j.toxicon.2015.11.015.

References

Alonso, R., Crawford, A.J., Bermingham, E., 2012. Molecular phylogeny of an endemic radiation of Cuban toads (Bufonidae: *Peltophryne*) based on mitochondrial and nuclear genes. J. Biogeogr. 39, 434–451.
Alonso, R., Del Castillo, S.D., Torres, E.L.M., García, L.Y., 2014. El anfibio endémico cubano de mayor talla: Conciliando récords, literatura y colecciones. Rev. Cuba. Cien. Biol. 3, 60–64.
Bagrov, A.Y., Fedorova, O.V., Dmitrieva, R.I., Howald, W.N., Hunter, A.P., Kuznetsova, E.A., Shpen, V.M., 1998. Characterization of a urinary bufodienolide Na+/K+-ATPase. Inhibitor in patients after acute myocardial infarction. Hypertension 31, 1097–1103.
Chan, W.Y., Ng, T.B., Yeung, H.W., 1995. Examination for toxicity of a Chinese drug, the total glandular secretion product Chan SU in pregnant mice and embryos. Biol. Neonate 67, 376–380.
Chen, K.K., Chen, A.L., 1933. Notes on the poisonous secretions of twelve species of toads. J. Pharmacol. Exp. Ther. 47, 281–293.
Chen, H., Meng, Y.H., Guo, D.A., Liu, X., Liu, J.H., Hu, L.H., 2015. New cytotoxic 19-norbufadienolide and bufogargarizin isolated from Chan Su. Fitoterapia 104, 1–6.
Cunha-Filho, G.A., Resck, I.S., Cavalcanti, B.C., Pessoa, C.Ó., Moraes, M.O., Ferreira, J.R.O., Rodrigues, F.A.R., dos Santos, M.L., 2010. Cytotoxic profile of natural and some modified bufadienolides from toad *Rhinella schneideri* parotoid gland secretion. Toxicon 56, 339–348.
Cunha-Flho, G.A., Schwartz, C.A., Resck, I.S., Murta, M.M., Lemos, S.S., Castro, M.S., Kyaw, C., Pires Jr., O.P., Leite, J.R.S., Bloch Jr., C., Schwartz, E.F., 2005. Antimicrobial activity of the bufadienolides marinobufagin and telocinobufagin isolated as major components from skin secretion of the *Bufo rubescens*. Toxicon 45, 777–782.
Daly, J.W., 1998. Thirty years of discovering arthropod alkaloids in amphibian skin. J. Nat. Prod. 61, 162–172.
Daly, J.W., Noimai, N., Kongkathip, B., Kongkathip, N., Wilham, J.M., Garraffo, H.M., Kaneko, T., Spande, T.F., Nimit, Y., Nabhitabhata, J., Chan-Ard, T., 2004. Biologically active substances from amphibians: preliminary studies on anurans from twenty-one genera of Thailand. Toxicon 44, 805–815.
Díaz, L.M., Cádiz, A., 2008. Guía taxonómica de los anfibios de Cuba. ABC Taxa 4, 1–294.
Estrada, A.R., Ruibal, R., 1999. A review of Cuban herpetology. In: Crother, B.L. (Ed.), Caribbean Amphibians and Reptiles. Academic Press, San Diego, pp. 31–62.
Evans, W.C., 2002. Saponins, cardiac drugs and other steroids. In: Saunders, W.B. (Ed.), Trease and Evans Pharmacognosy, pp. 289–314. London.
Ferreira, P.M.P., Lima, D.J.B., Debiasi, B.W., Soares, B.M., da Conceição Machado, K., da Costa, J.N., Rodrigues, D.J., Paulo, A.S., Pessoa, C., Magela- Vieira Jr., G., 2013. Antiproliferative activity of *Rhinella marina* and *Rhaebo guttatus* venom extracts from Southern Amazon. Toxicon 72, 43–51.
Fiske, C.H., Subbarow, Y., 1925. The colorimetric determination of phosphorus. J. Biol. Chem. 66, 375–392.
Fitch, R.W., Spande, T.F., Garraffo, H.M., Yeh, H.J., Daly, J.W., 2010. Phantasmidine: an epibatidine congener from the ecuadorian poison frog *Epipedobates anthonyi*. J. Nat. Prod. 73, 331–337.
Gao, H., Zehl, M., Leitner, A., Wu, X., Wang, Z., Kopp, B., 2010. Comparison of toad venoms from different *Bufo* species by HPLC and LC-DAD-MS/MS. J. Ethnopharmacol. 131, 368–376.
Henderson, R.W., Powell, R., 2009. Natural History of West Indian Reptiles and Amphibians. University Press of Florida, Gainesville, Florida.
Hutchinson, D.A., Savitzky, A.H., Burghardt, G.M., Nguyen, C., Meinwald, J., Schroeder, F.C., Mor, A., 2013. Chemical defense of an Asian snake reflects local availability of toxic prey and hatchling diet. J. Zool. 289, 270–278.
Jared, S.G.S., Antoniazzi, M.M., Jordao, A.E.C., Silva, J.R.M.C., Greven, H., Rodrigues, M.T., 2009. Parotoid macroglands in toad (*Rhinella jimi*): their structure and functioning in passive defense. Toxicon 54, 197–207.

Jing, J., Ren, W.C., Li, C., Bose, U., Parekh, H.S., Wei, M.Q., 2013. Rapid identification of primary constituents in parotoid gland secretions of the Australian cane toad using HPLC/MS-Q-TOF. Biomed. Chromatogr. 27, 685–687.
Kamano, Y., Kotake, A., Takano, R., Morita, H., Takeya, K., Itokawa, H., 1998. Conformational preference of two toad poison bufadienolides bufarenogin and ψ-bufarenogin. Heterocycles 49, 275–279.
Kamboj, A.J., Rathour, A., Kaur, M., 2013. Bufadienolides and their medicinal utility: a review. Intern. J. Pharm. Pharm. Sci. 5, 20–27.
Laursen, M., Yatime, L., Nissen, P., Fedosova, N.U., 2013. Crystal structure of the high affinity Na+K+-ATPase-ouabain complex with Mg2+ bound in the cation binding site. Proc. Natl. Acad. Sci. U. S. A. 110, 10958–10963.
Laursen, M., Gregersen, J.L., Yatime, L., Nissen, P., Fedosova, N.U., 2015. Structures and characterization of digoxin- and bufalin-bound Na+,K+-ATPase compared with the ouabain-bound complex. Proc. Natl. Acad. Sci. U. S. A. 112, 1755–1760.
Lee, S., Lee, Y., Choi, Y.J., Han, K.S., Chung, H.W., 2014. Cyto-genotoxic effects of the ethanol extract of Chan Su, a traditional Chinese medicine, in human cancer cell lines. J. Ethnopharmacol. 152, 372–376.
Li, B.J., Tian, H.Y., Zhang, D.M., Lei, Y.H., Wang, L., Jiang, R.W., Ye, W.C., 2015. Bufadienolides with cytotoxic activity from the skins of *Bufo bufo gargarizans*. Fitoterapia 105, 7–15.
Liu, Y.F., Feng, J.T., Xiao, Y.S., Guo, Z.M., Zhang, J., Xue, X.Y., Ding, J., Zhang, X.L., Liang, X.M., 2010. Purification of active bufadienolides from toad skin by preparative reversed-phase liquid chromatography coupled with hydrophilic interaction chromatography. J. Sep. Sci. 33, 1487–1494.
Lopez, L.B., Quintas, L.E.M., Noël, F., 2002. Influence of development on Na+/K+-ATPase expression: isoform- and tissue-dependency. Comp. Biochem. Phys. A 131, 323–333.
Low, B.S., 1972. Evidence from parotoid-gland secretions. In: Blair, W.F. (Ed.), Evolution in the Genus *Bufo*. Univ. Texas Press, Austin, Texas, pp. 244–264.
Lowry, O.H., Rosebrough, N.J., Farr, A.L., Randall, R.J., 1951. Protein measurement with the folin phenol reagent. J. Biol. Chem. 193, 265–275.
Mailho-Fontana, P.L., Antoniazzi, M.M., Toledo, L.F., Verdade, V.K., Sciani, J.M., Rodrigues, M.T., Jared, C., 2014. Passive and active defense in toads: the parotoid macroglands in *Rhinella marina* and *Rhaebo guttatus*. J. Exp. Zool. A 321, 65–77.
Mebs, D., Wagner, M.G., Pogoda, W., Maneyro, R., Kwet, A., Kauert, G., 2007. Lack of bufadienolides in the skin secretion of red bellied toads, *Melanophryniscus* spp. (Anura, Bufonidae), from Uruguay. Comp. Biochem. Phys. C 144, 398–402.
Moreno, Y., Banuls, L., Urban, E., Gelbcke, M., Dufrasne, F., Kopp, B., Kiss, R., Zehl, M., 2013. Structure-activity relationship analysis of bufadienolide-induced in vitro growth inhibitory effects on mouse and human cancer cells. J. Nat. Prod. 76, 1078–1084.
Mulholland, D.A., Schwikkard, S.L., Crouch, N.R., 2009. The chemistry and biological activity of the Hyacinthaceae. Nat. Prod. Rep. 30, 1165–1210.
Pôças, E.S., Touza, N.A., da Silva, A.J., Costa, P.R., Noël, F., 2007. Synergistic interaction between ouabain and 8-metoxy-3,9-dihydroxy coumestan, a non-steroidal synthetic inhibitor of Na+,K+-ATPase. Life Sci. 81, 1199–1204.
Qi, J., Tan, C.K., Hashimi, S.M., Zulfiker, A.H.M., Good, D., Wei, M.Q., 2014. Toad glandular secretions and skin extractions as anti-inflammatory and anticancer agents. Evid. Based Complement. Altern. Med. 1–9. http://dx.doi.org/10.1155/2014/312684.
Quintas, L.E.M., Lopez, L.B., Souccar, C., Noël, F., 1997. Na+/K+-ATPase density is sexually dimorphic in the adult rat kidney. Ann. N. Y. Acad. Sci. 834, 552–554.
Rash, L.D., Morales, R.A.V., Vink, S., Alewood, P.F., 2011. De novo sequencing of peptides from the parotid secretion of the cane toad, *Bufo marinus (Rhinella marina)*. Toxicon 57, 208–216.
Schmeda-Hirschmann, G., Quispe, C., Theoduloz, C., de Sousa Jr., P.T., Parizotto, C., 2014. Antiproliferative activity and new argininyl bufadienolide esters from the "cururú" toad *Rhinella (Bufo) schneideri*. J. Ethnopharmacol. 155, 1076–1085.
Schwartz, A., 1960. The large toads of Cuba. Proc. Biol. Soc. Wash. 73, 45–56.
Sciani, J.M., Angeli, C.B., Antoniazzi, M.M., Jared, C., Pimenta, D.C., 2013. Differences and similarities among parotoid macrogland secretions in South American toads: a preliminary biochemical delineation. Sci. World J. http://dx.doi.org/10.1155/2013/937407.
Slingerland, M., Cerella, C., Guchelaar, H.J., Diederich, M., Gelderblom, H., 2013. Cardiac glycosides in cancer therapy: from preclinical investigations towards clinical trials. Investig. New. Drug 31, 1087–1094.
Steyn, P.S., Heerden, F.V., 1998. Bufadienolides of plant and animals origin. Nat. Prod. Rep. 15, 397–413.
Takai, N., Kira, N., Ishii, T., Yoshida, T., Nishida, M., Nishida, Y., Nasu, K., Narahara, H., 2012. Bufalin, a traditional oriental medicine, induces apoptosis in human cancer cells. Asian Pac J. Cancer Prev. 13, 399–402.
Tempone, A.G., Carvalho Pimenta, D., Lebrun, I., Sartorelli, P., Taniwaki, N.N., Franco de Andrade Jr., H., Antoniazzi, M.M., Jared, C., 2008. Antileishmanial and antitrypanosomal activity of bufadienolides isolated from the toad *Rhinella jimi* parotoid macrogland secretion. Toxicon 52, 13–21.
Tian, H.Y., Luo, S.H., Liu, J.S., Wang, L., Wang, Y., Zhang, D.M., Zhang, X.Q., Jiang, R.W., Ye, W.C., 2013. C23 steroids from the venom of *Bufo bufo gargarizans*. J. Nat. Prod. 76, 1842–1847.
Toledo, R.C., Jared, C., 1995. Cutaneous granular glands and amphibian venoms. Comp. Biochem. Physiol. 111, 1–29.
Touza, N.A., Pôças, E.S., Quintas, L.E., Cunha-Filho, G., Santos, M.L., Noël, F., 2011. Inhibitory effect of combinations of digoxin and endogenous cardiotonic steroids on Na+/K+-ATPase activity in human kidney membrane preparation. Life Sci. 88, 39–42.
Van Bocxlaer, I., Loader, S.P., Roelants, K., Biju, S.D., Menegon, Bossuyt, F., 2010. Gradual adaptation toward a range-expansion phenotype initiated the global radiation of toads. Science 327, 679–682.
Wang, D., Bi, Z., 2014. Bufalin inhibited the growth of human osteosarcoma MG-63 cells via down-regulation of Bcl-2/Bax and triggering of the mitochondrial pathway. Tumor Biol. 35, 4885–4890.
Ye, M., Guo, D., 2005. Analysis of bufadienolides in the Chinese drug ChanSu by high-performance liquid chromatography with atmospheric pressure chemical ionization tandem mass spectrometry. Rapid Commun. Mass Spectrom. 19, 1881–1892.
Ye, M., Guo, H., Guo, H., Han, J., Guo, D., 2006. Simultaneous determination of cytotoxic bufadienolides in the Chinese medicine ChanSu by high-performance liquid chromatography coupled with photodiode array and mass spectrometry detections. J. Chromatogr. B 838, 86–95.
Zhang, H., Su, Y., Yang, F., Zhao, Z., Gao, X., 2014. Two new bufadienolides and one new pregnane from *Helleborus thibetanus*. Phytochem. Lett. 10, 164–167.